

# A Study of the Pressuremeter Modulus and Its Comparison to the Elastic Modulus of Soil

A. Fawaz<sup>1</sup>, F. Hagechade<sup>2</sup>, E. Farah<sup>3</sup>

<sup>1,2</sup>Université Libanaise, Institut Universitaire de Technologie (Saida) & Ecole Doctorale des Sciences et Technologies, Centre de Modélisation, PRASE, Beyrouth, Liban

<sup>3</sup>Université Libanaise, Ecole Doctorale des Sciences et Technologies, Centre de Modélisation, PRASE, Beyrouth, Liban

\*<sup>1</sup>alifawaz2014@gmail.com; <sup>2</sup>fadihagechade@hotmail.com; <sup>3</sup>elias\_farah@live.com

Received 4 July 2013; Accepted 11 December 2013; Published 25 March 2014

© 2014 Science and Engineering Publishing Company

## Abstract

Pressuremeter tests are conducted in many types of soil, in boreholes drilled at different locations and to several depths. Samples of encountered soil are taken and tested in the laboratory. Numerical simulations of the pressuremeter tests are performed with Plaxis software. The results allow the determination of the elastic modulus of soil and the comparison to the corresponding pressuremeter modulus measured during the in-situ tests. For every type of soil, the variation of the ratio between both moduli is determined.

## Keywords

*Pressuremeter; Soil; Numerical Simulation; Modulus; Borehole*

## Introduction

The pressuremeter test was developed by Louis Menard in 1957. This in-situ test provides the measurement of stress-strain response of soils. It is also used to evaluate the bearing capacity of soil foundations and the expected settlements (Baguelin et al. 1978). The pressure-volume curve obtained from this test is used to compute the pressuremeter modulus  $E_M$ . It is determined on the quasi-linear part of this curve within an interval defined by two specific pressure values:  $P_0$  which is roughly equivalent to the horizontal earth pressure at rest and the pressuremeter creep pressure  $P_f$ . However, this modulus differs from the elastic modulus  $E$  which is a principal soil parameter. The pressuremeter modulus value and the deduction of the elastic modulus from the pressuremeter test remain objects of discussion and researches (Gambin et al. 1996). The pressuremeter modulus has been related empirically to the elastic modulus of the soil as  $E_M/E = \alpha$ , (Menard, 1965), in which  $\alpha$  is termed by Menard as the rheological coefficient and has a value between 0 and 1.

Combarieu and Canépa (2001) mentioned that it is slightly complex to derive a modulus from the response of unload-reload cycles in a real pressuremeter test. Goh et al. (2012) proposed a correlation between the pressuremeter modulus and the SPT-N value.

The development of numerical methods allowed looking for other ways to extract Young's modulus from pressuremeter tests (Biarez et al. 1998) and deduce the shear resistance of soil (Shahrour et al., 1995; Fawaz et al., 2002).

In this paper, we present the results of a series of in situ pressuremeter tests at different depths. Soil samples are taken and tested in the laboratory. Pressuremeter tests are numerically simulated using Plaxis software to deduce the elastic modulus and compared to the pressuremeter one. The numerical results are compared to the experimental laboratory ones from one hand, and to analytical studies from the other hand. These results are finally grouped according to the soil type, in order to propose a ratio between the pressuremeter modulus and the elastic one for the soil types tested.

## Methodology

In order to cover various types of soil, 10 boreholes are drilled at 3 different sites in Lebanon and to several depths. Pressuremeter tests are performed in these boreholes at 2 m intervals, and soil samples are taken and tested in the laboratory. Experimental pressuremeter tests are numerically simulated using Plaxis software. Figure 1 shows the geometry model, the boundary conditions and the appropriate mesh used in the numerical study that simulates the real in-situ

conditions. The model has a width of 7m. The pressure is applied at the same depth of the experimental test to simulate the pressuremeter probe which is taken at 7 m from the bottom of the model. Since the problem is axisymmetric, a two-dimensional model is suitable to simulate the in-situ pressuremeter test.

The aim of this numerical study is the identification of the soil parameters using experimental test results. This involves choosing, as an initial step, the first entered values of soil parameters according to the soil type, and changing gradually these parameters, to reproduce by this numerical analysis, a calculated pressuremeter curve close as possible to the measured experimental one. This procedure allows the determination of the soil parameters: The elastic or Young's modulus  $E$ , the cohesion  $C$  and the internal friction angle  $\phi$ .

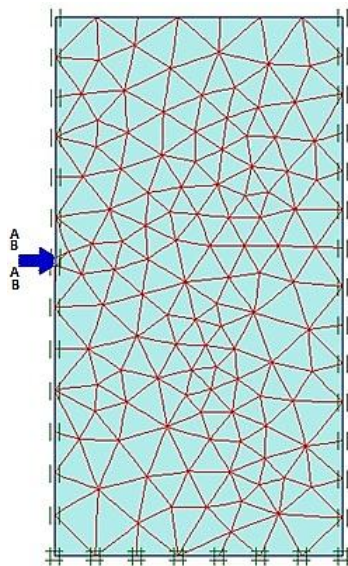


FIGURE 1 GEOMETRY of AXISYMMETRIC MODEL

Experimental Tests

Before computing numerically the elastic modulus, we present as follows the results of experimental tests from 10 boreholes executed in 3 different sites. Soil samples also taken from these boreholes have been tested in the laboratory to deduce the classification of soil layers according to the Unified Soil Classification System (USCS) as described in table I. Results of identification tests such as Sieve analysis and Atterberg limits provide an idea about the ranges of  $C$  and  $\phi$ .

Seven series of pressuremeter tests were realized in a mountain site near of Daher Elbaidar in Lebanon at 2 m intervals from the depth of 2 m to a depth varying from 21 to 48 m respectively. The first four boreholes show the existence of two principal layers: a mix of

clay and gravels and cobbles of limestone, and another layer of gravelly marl intercalated by sand, and by some gravelly sand and clay layers. The borehole N°5 indicates that the terrain is composed of a gravelly clay, marl and gravelly marl layers. The soil extracted from the borehole N°6 shows the existence of a gravelly and sandy clay layer and two layers of clay and sand. The borehole N°7 reveals that the soil is principally formed by a clayey sands and gravels layer.

The second site is located at Bekaa, Lebanon. Two series of pressuremeter tests are executed at this site proceeding from 2 m down to the depth of 26 and 28 m respectively. The summary tests for borehole drilled in this site detect the predominance of a clay layer.

TABLE 1 DISTRIBUTION OF SOIL LAYERS WITH DEPTH AND SOIL USCS CLASSIFICATION

Bore-holes	Depth	Identification (USCS)	Layers
N°1	0 to 10 m		Mix of clay, gravels and cobbles of limestone
	10 to 21 m	CL	Gravelly marl
	21 to 25 m	GC	
	25 to 33.5 m	CL	
	33.5 to 53 m	SC, SM or GM	
N°2	0 to 10 m		Mix of clay, gravels and cobbles of limestone
	10 to 16 m	CL	Sand
	16 to 17 m	ML	
	17 to 50 m	CL	Gravelly marl
	50 to 54 m	SW-SM and SC	Gravelly sand
N°3	0 to 6 m		Gravelly marl
	6 to 8 m	CL	
	8 to 17 m	GC	
	17 to 21 m	CL	
N°4	0 to 9 m		Gravelly marl
	9 to 33.5 m	CL	Sand
	33.5 m to 37.5m	SC-SM	
	37.5 m to 43 m	CL	Clay
N°5	0 to 9 m	CL	Gravelly clay
	9 m to 24.5m		Marl and gravelly marl
N°6	0 to 6 m	CL	Gravelly and sandy clay
	6 to 8 m		Clay
	8 to 26 m		Gravelly marl
	26 to 28m	ML	Sand
28 to 28.5 m	SC		
N°7	0 to 15 m	SC	Clayey sands and gravels
	15 to 24 m	CL	
	24 to 38 m	GW-GC	
N°8	0 to 8 m		Clay
	8 to 14.7 m	CL	
	14.7 to 18.5 m	SC	
	18.5 to 26 m	CL	
N°9	0 to 5.5 m		Clay
	5.5 to 13 m	CL-ML	
	13 to 25 m	CL	
N°10	2 to 17 m	SM	Sand

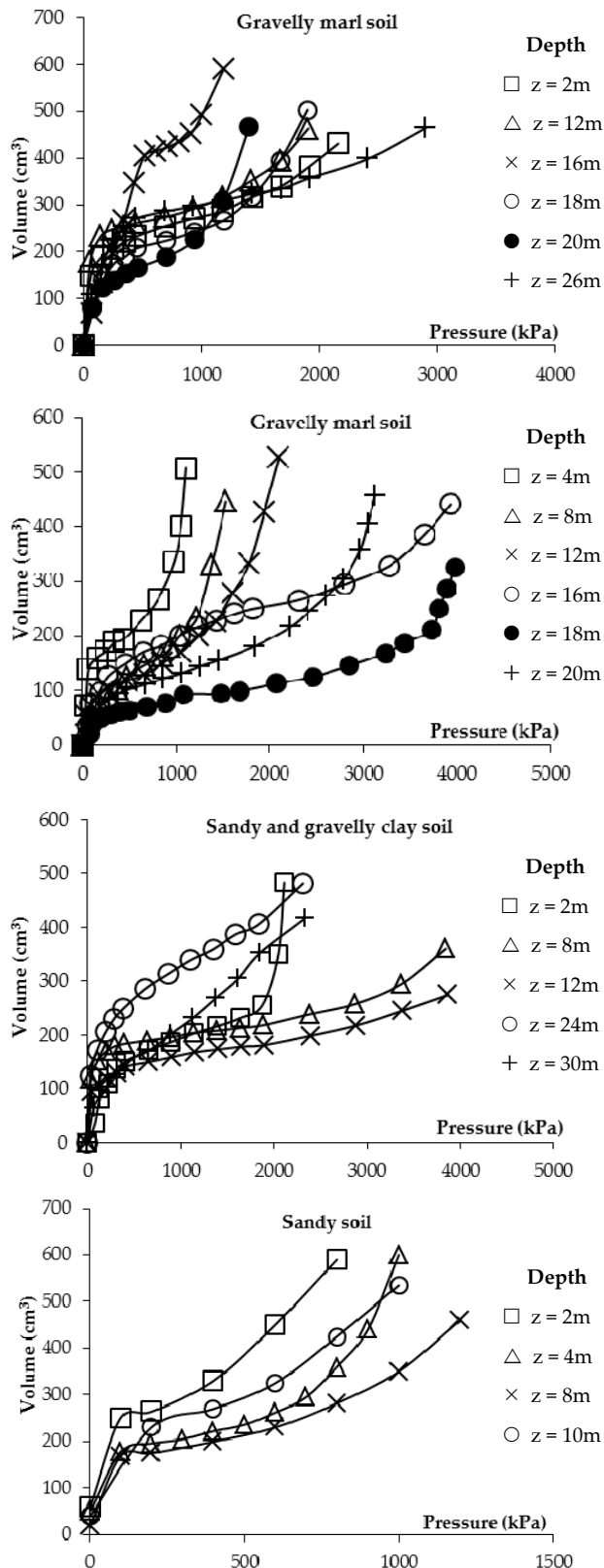


FIGURE 2 EVOLUTION OF EXPERIMENTAL PRESSUREMETER CURVES WITH DEPTHS

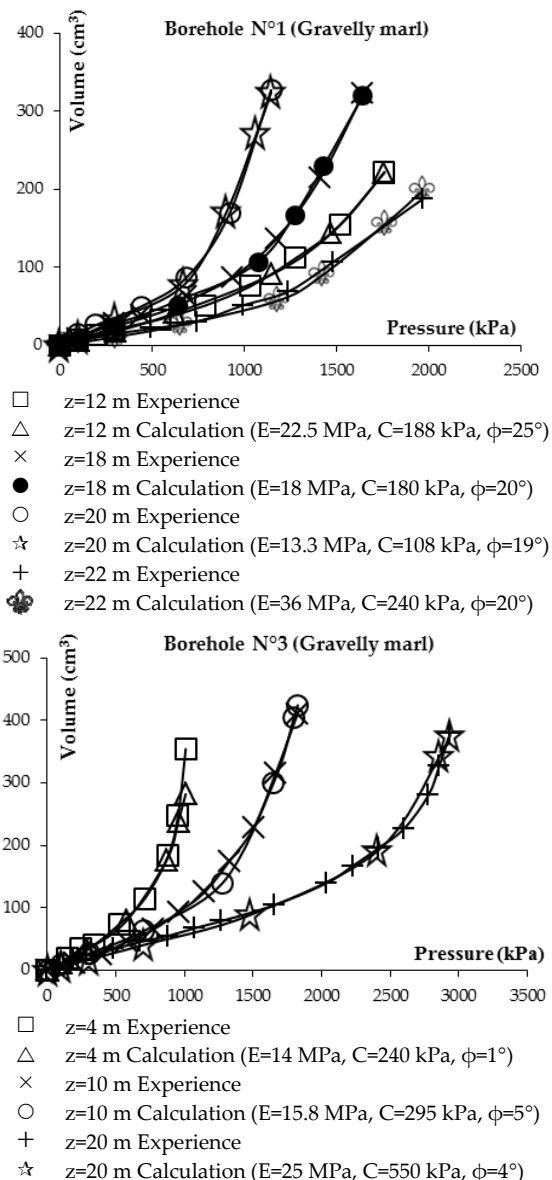
The third site is located in Beirut, Lebanon where a sandy soil is encountered. Figure 2 represents respectively the evolution of experimental pressure-volume curves with depths for boreholes N°1 (gravelly

marl soil), N°3 (gravelly marl soil), N°6 (sandy and gravelly clay soil) and N°10 (sandy soil). Table 1 summarizes the description and the classification of the soil layers encountered in the ten boreholes.

Numerical Analysis

Applying the methodology of the numerical analysis described above, we have simulated the pressuremeter test for the ten boreholes at different depths. As soil's behavior, we have used a Mohr-Coulomb model with a Poisson ratio  $\nu = 0.33$ . Three parameters are unknown: the elastic modulus  $E$ , the cohesion  $C$  and the friction angle  $\phi$ .

Starting with a first combination of these three parameters according to the soil type at the test depth, the pressuremeter modulus  $E_M$  can be used as the first input.



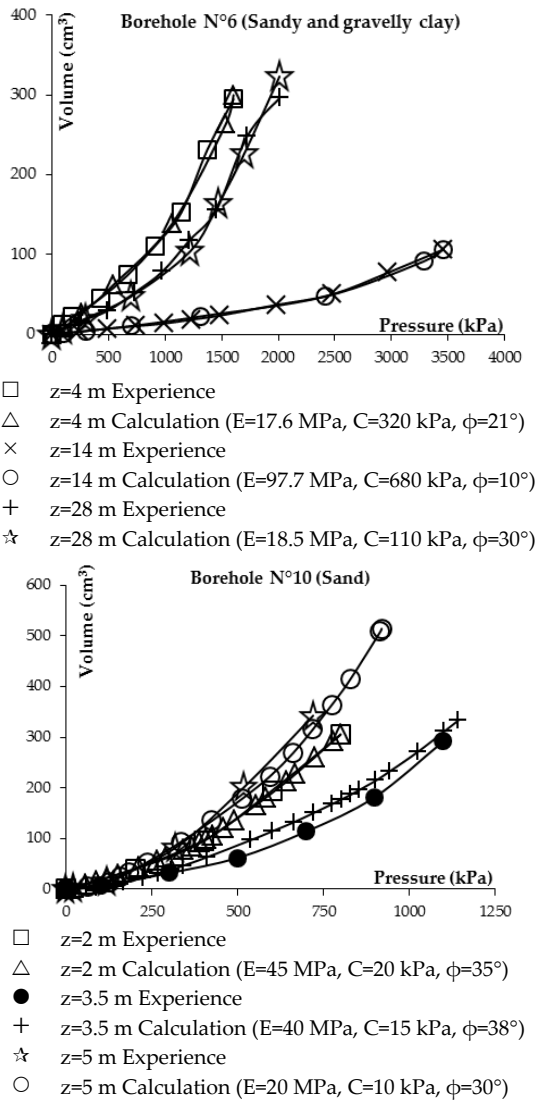


FIGURE 3 EXPERIMENTAL AND NUMERICAL PRESSURE-VOLUME CURVES AT DIFFERENT DEPTHS

We change the values of these parameters to reproduce by the numerical way the experimental pressuremeter curve. Then special attention is paid to that the two slopes of the experimental and numerical curves in the elastic phase should be similar.

Figure 3 shows some examples of comparison between the calculated pressuremeter curve and the experimental one at some depths for the borehole N°1, N°3, N°6 and N°10 respectively, noting that, the point (P<sub>0</sub>, V<sub>0</sub>) is taken as origin of the axis.

The calculated curves are close to the experimental one to allow the deduction of the characterization of the soil layers and the determination of the three mechanical parameters: E, C, and φ. Noting that changing the values of the cohesion and the friction angle in an opposite and remarkable manner leads to a numerical curve that doesn't match the experimental one. In order to compare numerical and analytical results, it is essential to mention the theoretical study used to

determine the mechanical parameters of soil.

Different rheological laws have been developed to describe the behavior of soils around the pressuremeter. The study of Combarieu (1995) based on Pasturel's formula has evolved a theoretical relation between the limit pressure P<sub>1</sub> and soil parameters E, ν, C and φ. In case of cohesive and granular soils (C and φ different to 0) that relation is:

$$P_1 + c \cot \varphi = (P_0 + c \cot \varphi)(1 + \sin \varphi) \left[ \frac{E}{2(1 + \nu)(P_0 + c \cot \varphi) \sin \varphi} \right]^{\frac{\sin \varphi}{1 + \sin \varphi}}$$

According to this formula and using the values of the pressure at rest P<sub>0</sub> and limit pressure P<sub>1</sub> determined from the test in-situ and elastic modulus obtained in the numerical analysis, we calculate the cohesion and the friction angle.

TABLE 2 EXPERIMENTAL, NUMERICAL AND ANALYTICAL RESULTS FOR SANDY AND GRAVELLY CLAY

Sandy and gravelly Clay									
E <sub>M</sub> (MPa)	P <sub>0</sub> (kPa)	P <sub>1</sub> (kPa)	Numerical results			Analytical results		E <sub>M</sub> /P <sub>1</sub>	E <sub>M</sub> /E
			E (Mpa)	C (kPa)	φ°	C (kPa)	φ°		
4	159	672	5.5	90	2	115	4	5.95	0.73
11	165	2200	12.4	430	10	539	14	5.00	0.89
40	676	4300	63	800	20	604	19	9.30	0.63
14.1	200	1804	17.5	320	21	232	18	7.82	0.81
24	350	2307	28.1	150	25	147	22	10.40	0.85
18	300	2500	20	290	25	278	25	7.20	0.90
14	300	2306	15	300	30	271	28	6.07	0.93

TABLE 3 EXPERIMENTAL, NUMERICAL AND ANALYTICAL RESULTS FOR CLAY

Clay									
E <sub>M</sub> (MPa)	P <sub>0</sub> (kPa)	P <sub>1</sub> (kPa)	Numerical results			Analytical results		E <sub>M</sub> /P <sub>1</sub>	E <sub>M</sub> /E
			E (Mpa)	C (kPa)	φ°	C (kPa)	φ°		
9	100	1108	14	240	1	240	1	8.12	0.64
7	76	960	8.5	220	1	242	1	7.29	0.82
11	276	2200	15.8	295	5	391	13	5.00	0.70
52	100	4400	95	680	7	685	9	11.82	0.55
32	299	3980	40	480	4	705	12	8.04	0.80
22	190	3150	25	550	4	710	9	6.98	0.88
27	165	1720	38	195	7	218	9	15.70	0.71
63.5	400	4100	73	650	2	700	4	15.49	0.87
85	400	4400	97.7	680	10	539	10	19.32	0.87
4	67	627	5.3	36	17	164	12	6.38	0.75
16	186	890	18	38	2	84	9	17.98	0.89
12	57	1550	14	180	2	385	7	7.74	0.86
11	81	1550	16	148	9	375	9	7.10	0.69
14	87	1450	17	145	3	342	3	9.66	0.82
11	576	2100	13	180	4	406	4	5.24	0.85

TABLE 4: EXPERIMENTAL, NUMERICAL AND ANALYTICAL RESULTS FOR CLAYEY SANDS AND GRAVELS

Clayey sand and gravels									
E <sub>M</sub> (MPa)	P <sub>0</sub> (kPa)	P <sub>1</sub> (kPa)	Numerical results			Analytical results		E <sub>M</sub> /P <sub>1</sub>	E <sub>M</sub> /E
			E (Mpa)	C (kPa)	φ°	C (kPa)	φ°		
1.24	68	400	1.45	120	19	103	16	3.10	0.86
3.89	147	604	4.1	140	20	61	15	6.44	0.95
1.39	61	302	1.5	60	17	47	17	4.60	0.93
3.7	157	700	4.1	175	17	86	16	5.29	0.90
10	100	1533	12.5	183	24	244	23	6.52	0.80
114.5	980	4200	120	176	13	32	17	27.26	0.95
17	400	2410	18.5	110	30	129	30	7.05	0.92
48	434	4000	51	180	25	400	20	12.00	0.94

TABLE 5 EXPERIMENTAL, NUMERICAL AND ANALYTICAL RESULTS FOR MARL

Marl									
E <sub>M</sub> (MPa)	P <sub>0</sub> (kPa)	P <sub>1</sub> (kPa)	Numerical results			Analytical results		E <sub>M</sub> /P <sub>1</sub>	E <sub>M</sub> /E
			E (Mpa)	C (kPa)	φ°	C (kPa)	φ°		
14	278	2150	16	160	16	291	20	6.51	0.88
40	180	2690	48	138	22	241	21	14.87	0.83
41	864	4290	50.2	450	17	342	15	9.56	0.82
13	104	1522	13.1	85	23	232	24	8.54	0.99

TABLE 6 EXPERIMENTAL, NUMERICAL AND ANALYTICAL RESULTS FOR GRAVELLY MARL

Gravelly marl									
E <sub>M</sub> (MPa)	P <sub>0</sub> (kPa)	P <sub>1</sub> (kPa)	Numerical results			Analytical results		E <sub>M</sub> /P <sub>1</sub>	E <sub>M</sub> /E
			E (Mpa)	C (kPa)	φ°	C (kPa)	φ°		
21.3	148	2100	22.5	188	25	238	26	10.14	0.95
5.3	253	1000	5.5	110	22	103	17	5.30	0.96
17.7	257	2000	18	180	20	221	21	8.85	0.98
13.3	263	1480	13.3	108	19	131	19	8.99	1.00
29.6	440	2600	30	210	25	238	16	11.38	0.99
14.6	456	2250	15	110	18	217	20	6.49	0.97
14	448	2250	15	220	18	250	18	6.22	0.93
18.9	348	1960	20	225	16	201	15	9.64	0.95
20	450	2250	20	185	21	170	19	8.89	1.00
83	934	3550	83	280	14	197	10	23.38	1.00
31.3	462	2550	34	95	12	160	18	12.27	0.92
23.28	262	1960	40	188	14	180	13	11.88	0.58
20.59	270	2096	24.8	255	8	294	11	9.82	0.83
5.36	150	1412	5.6	170	15	400	17	3.80	0.96
25.85	360	2398	28	280	10	300	12	10.78	0.92
28	500	3906	35	650	5	667	10	7.17	0.80
19.45	800	3146	21.3	200	20	182	20	6.18	0.91
130.4	852	4900	142.8	86	9	250	13	26.61	0.91

TABLE 7 EXPERIMENTAL, NUMERICAL AND ANALYTICAL RESULTS FOR SAND

Sand									
E <sub>M</sub> (MPa)	P <sub>0</sub> (kPa)	P <sub>1</sub> (kPa)	Numerical results			Analytical results		E <sub>M</sub> /P <sub>1</sub>	E <sub>M</sub> /E
			E (Mpa)	C (kPa)	φ°	C (kPa)	φ°		
12	200	1200	45	20	35	13	20	10.00	0.27
23	100	1100	40	10	28	14	29	20.91	0.58
26	100	1300	40	15	38	14	18	20.00	0.65
18	100	1200	20	10	30	31	38	15.00	0.90
77	150	Not reached	120	36	45	-	-	-	0.64
112	146	Not reached	250	20	40	-	-	-	0.45

Results

All results have been regrouped according to soil type encountered in the 3 tested sites. We distinguish 6 types: clay, sandy and gravelly clay, clayey sand and gravels, gravelly marl, marl and sand. Tables 2, 3, 4, 5, 6 and 7 show experimental, numerical and analytical results grouped by the type of materials in addition to the ratio of the pressuremeter modulus over the limit pressure and the elastic modulus.

Synthesis of the Results

The tables shown above summarize all results obtained at three different sites regrouped according to the type of soils. Menard proposed the ratio of  $E_M/E$  is between 0 and 1, this ratio is retrieved by the results of

the numerical simulations of the pressuremeter test, and also a reduction of this interval for some types of soils has been occurred as follows:

- Clay:  $0.55 < \alpha < 1$
- Sandy and gravelly clay:  $0.6 < \alpha < 1$
- Clayey sand and gravels:  $0.8 < \alpha < 1$
- Gravelly marl:  $0.55 < \alpha < 1$
- Marl:  $0.8 < \alpha < 1$
- Sand:  $0.25 < \alpha < 1$

Figure 4 represents the variation of the pressuremeter modulus in function of the net limit pressure  $P_1^*$  which is the difference between the limit pressure and the horizontal earth pressure at rest. It is clear that  $E_M$  varies gradually with the limit pressure.

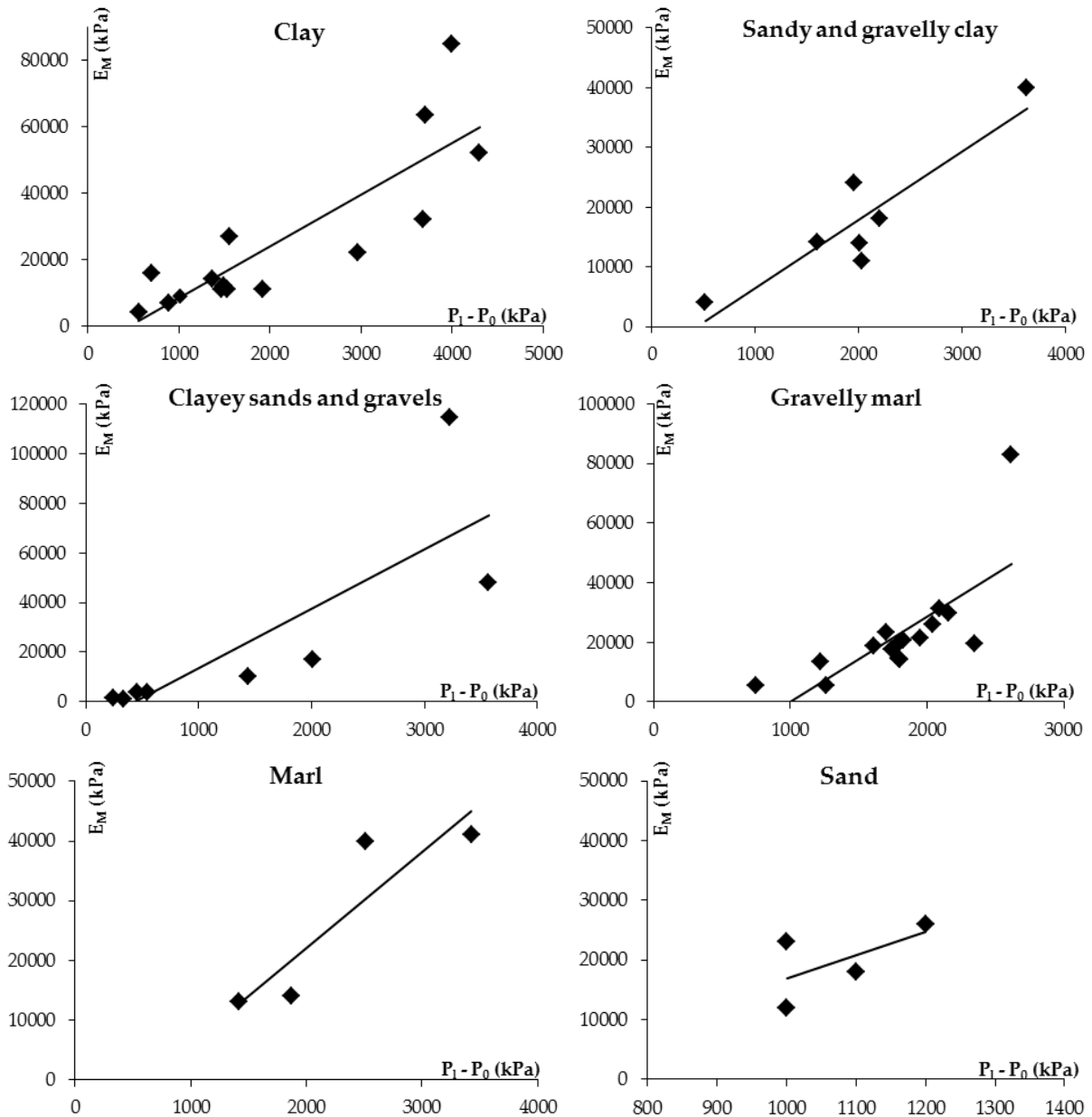


FIGURE 4 VARIATION OF  $E_m$  IN FUNCTION OF  $P_1 - P_0$

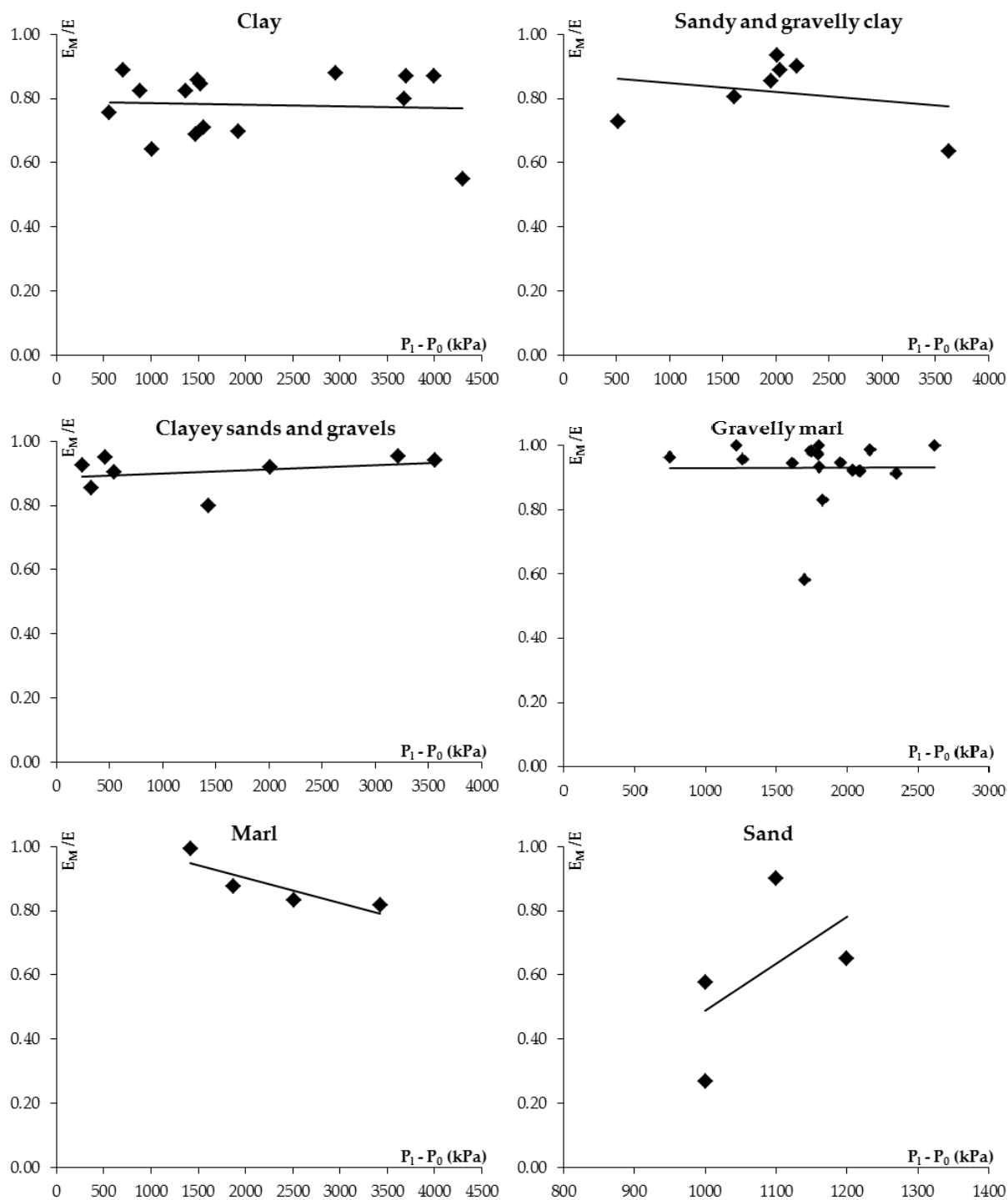


FIGURE 5 VARIATION OF  $E_M/E$  IN FUNCTION OF  $P_1 - P_0$

Figure 5 shows the evolution of the ratio  $E_M/E$  of the pressuremeter modulus over the elastic one in function of the net limit pressure  $P_1^*$ . These curves confirm the classification listed above.

Figure 6 represents the variation of the elastic modulus  $E$  with the shear resistance  $\tau = c + \sigma \tan \phi$ , where  $c$  and  $\phi$  are the soil parameters computed numerically and  $\sigma$  is the vertical stress. Figure 7 shows the evolution of the limit pressure with the shear resistance. Each curve

corresponds to the appropriate soil type.

The elastic modulus introduced in the computations can be calculated by considering the soil elasticity with a lower bound deformation magnitude. On the numerical pressuremeter curves, the moduli were computed as if they were measured in real tests. They correspond to a deformation magnitude ranging between  $10^{-2}$  and  $10^{-1}$ .

Soil samples tested in the laboratory are at some

depths subjected to the shear box test to determine the shear resistance of soil. The values of the friction angle computed numerically are very close even similar to those measured in the laboratory. The calculated values of cohesion differ sometimes from those determined from the shear box test due to the disturbance of tested soil samples. Soil parameters calculated using the analytical method and the elastic modulus calculated numerically are close to the numerical ones. This confirms the validity of the proposed numerical methodology.

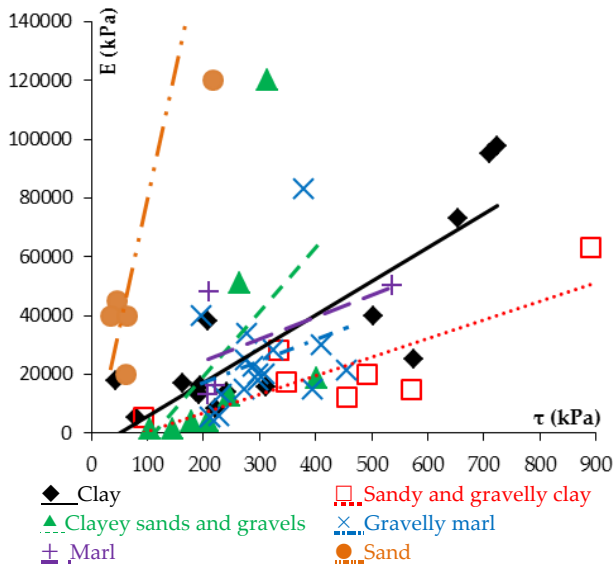


FIGURE 6 VARIATION OF ELASTIC MODULUS WITH SHEAR STRESS

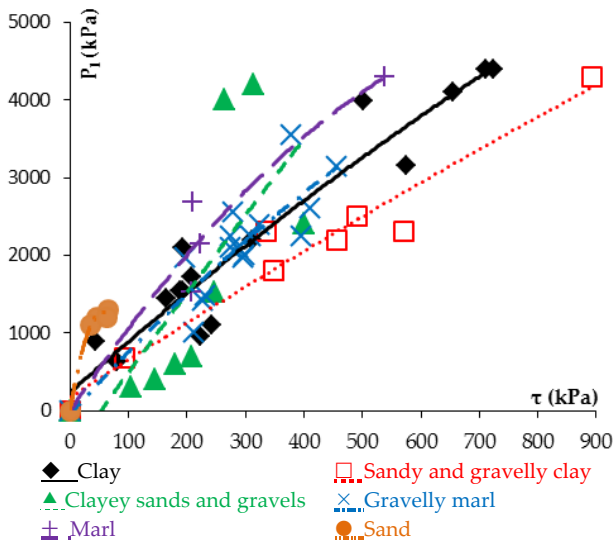


FIGURE 7 VARIATION OF LIMIT PRESSURE WITH SHEAR STRESS

Conclusion

The design of any structure or foundation requires a good understanding of the underlying ground condition. One of the most important parameters is the

elastic or Young's modulus. In this paper, several geotechnical studies have been presented in three sites with different soil types. Based on in-situ tests results, numerical simulations have been developed to extract soil parameters especially the elastic modulus compared to the pressuremeter one. The interval of values of the rheological coefficient  $\alpha = E_M/E$  proposed by Menard has been retrieved and reduced for the soil types tested.

REFERENCES

Baguelin F., Jézequel J.F., Shields D. H. "The pressuremeter and foundation engineering, series on rock and soil mechanics." Trans Tech Publications. Clausthal-Germany, (1978).

Biarez J., Gambin M., Gomes-Correia A., Flavigny E., Branque D. "Using pressuremeter to obtain parameters to elastic-plastic models for sands." Geotechnical Site Characterization, Robertson & Mayne, Balkema, Rotterdam, (1998).

Cambou B., Boubanga A., Bozett O.P., and Maghgo M., "Determination of constitutive parameters from pressuremeter tests." Third international symposium on pressuremeters. Oxford University 2-6 April, Thomas Telford ed., London, pp, 243-252, (1990).

Combarrieu O., Canépa Y. "The unload-reload pressuremeter test." Bulletin de des Laboratoires des Ponts et Chaussées 233, July – August pp. 37-67, (2001).

Combarrieu O. "L'essai pressiométrique et la résistance au cisaillement des sols." Bulletin de Liaison des Laboratoires des Ponts et Chaussées 196, Mars – Avril pp.43-50, (1995).

Fawaz A., Boulon M., Flavigny E. "Parameters deduced from the pressuremeter test." Canadian Geotechnical Journal, Volume 39, N° 6, pp. 1333-1340, (2002).

Gambin M., Flavigny E., Boulon M. "Le module pressiométrique." Historique et modélisation XI<sup>e</sup> Colloque Franco-Polonais de Mécanique des sols et des roches appliquées". Gdansk. September 1996, pp. 53-60.

Goh K.H., Jeyatharan K., Wen D. "Understanding the Stiffness of Soils in Singapore from Pressuremeter Testing." Geotechnical Engineering Journal of the SEAGS & AGSSEA Vol. 43 No. 4 December 2012.

Ménard, L. "Mesure in – situ des propriétés physiques des sols." Annales des ponts et chaussées. Vol 14, pp. 357 – 377, (1957).

Shahrour I., Kasdi A., Abriak N. "Utilisation de l'essai  
pressiométrique pour la détermination des propriétés  
mécaniques des sables obéissant au critère de Mohr-

Coulomb avec une règle d'écoulement non associée."  
Revue Française de Géotechnique, N° 73, pp. 27-33,  
(1995).